PHILOSOPHICAL TRANSACTIONS OF THE ROYAL SOCIETY A
MATHEMATICAL, PHYSICAL & ENGINEERING SCIENCES

Helium Line Emission: Its Relation to Atmospheric Structure

Carole Jordan

Phil. Trans. R. Soc. Lond. A 1980 **297**, 541-554
doi: 10.1098/rsta.1980.0230

Phil. Trans. R. Soc. Lond. A **297**, 541–554 (1980) [541]
Printed in Great Britain

Helium line emission: its relation to atmospheric structure

BY CAROLE JORDAN
Department of Theoretical Physics, 1 Keble Road, Oxford OX1 3NP, U.K.

[Plates 1 and 2]

A brief review is given of observations of the resonance lines of He I and He II and their interpretation. As discussed in a previous paper, the helium lines are anomalously strong in the quiet Sun when compared with other transition region lines. The enhancement can be brought about by the transient excitation of the lines by electrons of higher temperature than that which determines the ion population. The variation in the intensity of the helium lines relative to those of other transition region lines appears to be related to variations in the temperature gradient between different parts of the atmosphere. To relate the degree of enhancement to other observable parameters, such as electron pressure and absolute line intensities, and thus to the structure of the atmosphere, a method for analysing the emission measure distribution previously developed in the context of the quiet atmosphere and active region loops is applied also to coronal holes. It is proposed that the non-thermal ion motions observed in the transition region can provide the required mechanism for transporting the helium ions across the steep temperature gradient. By making a simple model, an expression is developed which relates the helium enhancement to the non-thermal motions, the transition region temperature gradient and the electron pressure. The scaling laws implied can be tested against further observations when they become available.

1. INTRODUCTION

The lines of He I and He II exhibit a behaviour that is quite different from that either of transition region lines or of coronal lines. The present paper is concerned with the underlying reasons for this behaviour.

In §2 a brief review is given of available observations and previous analyses. From these one can draw the broad conclusion that the helium emission is enhanced in regions where the temperature gradient is relatively steep, and is weak in regions known to have relatively gentle temperature gradients.

Since the helium emission apparently depends on the temperature gradient one of the aims of the present paper is to relate the degree of enhancement expected to the measurable atmospheric parameters. In particular, the helium emission enhancement is expressed in terms of the same parameters as used by Jordan (1975*a*, 1976) to describe the structure and energy balance of the quiet Sun and active region loops. These parameters are P_0, the pressure in the transition region, T_c, the coronal temperature, and a, which determines the absolute value of the emission measure at a given temperature. Before the helium emission is discussed, it is necessary to show how the method developed by Jordan can be applied also to coronal holes, and this is done in §3.

The relation between this work and that of Hearn (1975), who makes the hypothesis of minimum energy loss to derive scaling laws between P_0 and T_c, is discussed, since Hearn (1977) has applied his proposals in some detail to a coronal hole. Given the same assumption of minimum energy loss, the scaling laws deduced from the present work agree with those of Hearn.

Recent work on the energy balance of coronal structures (Jordan 1980) suggests that the observed non-thermal motions in the transition region are related to the energy conducted back from the corona, and hence to the temperature gradient. The possibility then arises that it is these non-thermal motions that are the cause of the helium enhancement, since they could provide the means by which helium ions are mixed with hotter electrons. An expression for the helium enhancement in terms of P_0, T_c, a and v_T, the non-thermal velocity at *ca.* 10^5 K, is developed in §4. There may be sufficient observations available to test the scaling laws proposed, but if so they do not seem to have been analysed yet in an appropriate form. It is hoped that this paper will stimulate further work in this area.

2. The He I and He II emission

It has been known for many years (Tousey 1967) that spectroheliograms of the whole Sun made in the resonance line of He II at 304 Å† show that the emission is lower in intensity in the polar regions. Early observations also showed (e.g. those of Reeves & Parkinson 1970; Tousey *et al.* 1973) that the emission from He I and He II is less intense in coronal holes observed on the disk, whereas the emission from other lines formed at similar temperatures in the transition region is not reduced in intensity. Simple calculations of the expected helium intensity as a function of temperature show that the 'coronal' contribution to the He I 584 Å and He II 304 Å lines is negligible, and other explanations are need to explain the anomalous behaviour of these lines.

Zirin (1969) proposed that this could be due to He II absorption in the corona, but later (Zirin 1975) revised his views and instead suggested that because of the importance of coronal extreme-ultraviolet emission in photo-ionizing He I and He II the reduction of coronal emission over coronal holes could explain the reduction in the helium line intensities.

Calculations of the helium line intensities, by using a variety of solar and excitation models, had been made previously (Athay & Johnson 1960; Athay 1960, 1965) but comparisons were not made with the intensities expected from other transition region lines, since suitable observational data did not exist. Both collisional excitation (Athay & Johnson 1960) and photo-ionization followed by recombination (Goldberg 1939) had been investigated. Hirayama (1971) has followed up the radiative model, mainly in the context of prominences which will not be discussed in this paper.

Hearn (1969*a*) made extensive calculations of the intensities of the He I lines at 584 and 537 Å and of their dependence on N_e and T_e, including both collisional and radiative processes. The lines of He II were treated in a second paper (Hearn 1969*b*). Although the solutions, in terms of density and temperature, that could fit the observation were considered, no comparison was made with other transition region lines, or with specific models.

Milkey *et al.* (1973) calculated the emission expected from He I 584 Å, using the solar model of Vernazza *et al.* (1973). They found that the model gave an emission which was a factor of three lower than that observed from the OSO-4 satellite (Dupree & Reeves 1971). Although photo-ionization by coronal radiation was found to play an important part in establishing the ionization equilibrium, it could not account for the strength of the resonance line. Milkey *et al.* suggested that the region around 45000 K needed to be thicker than in the model of

† 1 Å = 10^{-10} m = 10^{-1} nm.

Vernazza *et al.* Milkey (1975) disputed the explanation proposed by Zirin (1975) and pointed out that the profiles of the He I and He II resonance lines (Doschek *et al.* 1974; Feldman & Behring 1974; Cushman *et al.* 1975) did not show the central reversals expected in a photo-ionization recombination model.

Observations of the profile of the He II Balmer alpha line at 1640 Å (Feldman *et al.* 1975; Boland *et al.* 1975; Kohl 1977) indicate that a recombination component is present as well as one due to collisional excitation. The work by Kohl shows most clearly that narrow spectral features formed by recombination are present, superimposed on a broader profile formed by collisional excitation and non-thermal motions.

The most important aspect of the behaviour of the helium emission is that its observed intensity varies from place to place on the Sun in a manner that is quite different from that of other transition region lines. Thus it is not sufficient to compare the helium emission observed with that calculated from a particular model. The same model must be used to calculate the intensities of other transition region lines, and an explanation found for the variation in the relative intensities of these and the helium lines. Pottasch (1964) had made such a comparison, but the anomalous behaviour of helium was not apparent because of the less reliable intensities and atomic data then available.

Jordan (1975*b*) found that models that could satisfactorily account for the intensities of transition region lines underestimated the observed emission in He I and He II by factors of 15 and 5.5. The abundance of helium used is $N_{\mathrm{He}}/N_{\mathrm{H}} = 0.10$, which can be taken as an upper limit in view of observations of the solar wind which indicate an *average* of less than 0.055. Measurements from solar cosmic rays indicate more constant and slightly higher values, between 0.062 and 0.09. Models of the solar interior and upper limits to the solar neutrino flux suggest values of between 0.049 and 0.064. The above typical values are all taken from Hundhausen (1972) and the references cited there. By using Hearn's (1969*a*, *b*) calculations for the level populations as a function of temperature and density, no satisfactory solution for the absolute and relative intensities of the lines of He I and He II could be found that simultaneously agreed with the models derived from the transition region lines of other elements. It was proposed that instead of the lines being formed at the temperature expected in a state of ionization equilibrium, the excitation of the helium lines takes place by electrons of higher temperature than that appropriate to the ion population ratios. For example, a process that rapidly moves ions formed at one temperature to a region of higher temperature could allow excitation of the lines to take place before a new ionization equilibrium is reached. Alternatively, the local electron temperature could be raised in a transient manner. Such processes would increase the emission from the helium resonance lines without causing significant effects in other elements simply because of the sensitivity to temperature of the exponential term ($\exp(-W/kT_{\mathrm{e}})$) in the collisional excitation rate, W/kT_{e} being much larger for the helium lines than for typical transition region lines. (W is the excitation energy of the transition.) With T_{e} increased by a factor of two above that expected with equilibrium calculations, order of magnitude increases in the helium emission result.

The variation of the helium lines intensities, relative to other transition region lines, between the average Sun and coronal holes can be understood in terms of the lower temperature gradient in coronal holes, which would reduce the effectiveness of the type of mixing process suggested. Munro & Withbroe (1972) found that the temperature gradient in a coronal hole could be up to an order of magnitude lower than in the quiet Sun. The helium anomaly is therefore that the lines are *enhanced* in the quiet Sun, not that they are *reduced* in coronal holes. In general one would expect the degree of enhancement to be related to the temperature gradient in the transition region.

Shine *et al.* (1975) suggested that thermal diffusion, which would cause ions to be carried up the steep temperature gradient, might be the required process for mixing 'cool' ions with 'hotter' electrons.

Further calculations of He II line intensities were made by Linsky *et al.* (1976) and were compared with observations from the OSO-7 satellite. No comparison was made with other transition region lines. Apart from isothermal slab models, two models for the temperature and density structure of the atmosphere were used, based on combinations of the model by Vernazza *et al.* (1973) below *ca.* 30000 K and that of Dupree (1972) above 30000 K. In addition to the resonance line at 304 Å, detailed comparisons were made between the calculated and observed intensities of the He II continuum, and higher members of the He II Lyman series. For the 304 Å line, the results confirmed the earlier conclusions of Jordan using Hearn's calculations and intensities then available. The observed He II 304 Å line was found to be about a factor of six stronger than calculated.

Avrett *et al.* (1976) also treated the He I and He II continua and solved the He II 304 Å line transfer equation with an approximate calculation of the ionization equilibrium. They used as a model a combination of the model by Vernazza *et al.* (1973) and that defined by the emission measure distribution given by Jordan (1975*b*), with $P_e = 5.6 \times 10^{14}\ \mathrm{cm^{-3}\ K}$. The calculations by Avrett *et al.* led to conclusions agreeing with those of Milkey (1975), Milkey *et al.* (1973) and Linsky *et al.* (1976). The discrepancy between the observed and calculated intensities of the 304 Å line was found to be about a factor of three, lower than the previous value of six. The main reason for this difference between the results of Avrett *et al.* (1976) and Jordan (1975*b*) is that whereas Jordan assumed that only one-half of the created photons escape outwards, the detailed calculations give a greater fraction of photons escaping the atmosphere because of the higher opacity at lower temperatures.

The observed profiles of the 304 and 1640 Å lines in the quiet Sun are consistent with a model where the ion temperature is *ca.* 80000 K, and the non-thermal motions are *ca.* 25 km $\mathrm{s^{-1}}$ (typical of the quiet Sun values around 10^5 to 2×10^5 K).

In particular, Kohl (1977) showed that these conditions could satisfactorily fit the broad, collisionally excited component of the 1640 Å line. By using the same parameters the predicted width (f.w.h.m.) for the 304 Å line is only 0.058 Å, narrower than the observed value of *ca.* 0.11 Å. However, the calculations by Avrett *et al.* (1976), which include line broadening through trapping of resonance line photons, indicate that when this is taken into account the calculated width agrees well with that observed. (Jordan 1975*b*) did not allow for this broadening when discussing apparent problems with He II line widths.)

More recently, Mango *et al.* (1978) have used observations made with the Naval Research Laboratory's slitless spectrograph on Skylab to make a detailed study of the behaviour of the He I lines at 584 and 537 Å and the He II lines at 304 and 256 Å. The centre-to-limb behaviour was used to deduce differences in the temperature gradient between the quiet Sun and a coronal hole, and they found a lower temperature gradient in coronal holes. Although this work is clearly of long-term value, in that proposed models must match the observed behaviour of the lines, it is more immediately important for other transition region lines from the same regions to be studied simultaneously. It is the difference between the helium intensity predicted by models that fit the other transition lines and the observed helium intensity, that will give the strongest constraint on the enhancement mechanism. Otherwise, comparisons are heavily model dependent.

Many aspects of the He I and He II emission are shown very clearly in the observations, made from a Naval Research Laboratory rocket flight, reported by Brueckner & Bartoe (1974). These observations are in the form of whole Sun spectroheliograms and include regions of the quiet Sun, coronal holes, active regions and sunspots.

Brueckner & Bartoe give an extensive discussion of these observations and only those conclusions that relate to the helium emission will now be summarized.

Figure 1, plate 1, taken from Brueckner & Bartoe, shows that the weaker helium emission in coronal holes arises from a reduction in the intensity of the chromospheric network, compared with the quiet Sun. Such a reduction is not apparent in other transition region lines.

Figure 2, plate 2, shows active regions McMath 706 (upper left corner) and McMath 703 (lower right), and includes a sunspot in McMath 703. It can be seen that the He I and He II emission is very weak above the sunspot, while emission from O V and Ne VII is relatively strong. It can be seen that He II can be strong in regions where the broad-band coronal emission is relatively weak, indicating that the coronal radiation alone does not control the helium emission.

Brueckner & Bartoe point out that some small scale features in the active region show large line broadening in the O V image but not in the He I or Ne VII images. The broadening would correspond to velocities 150 km s^{-1}. It would be of interest to establish the behaviour of the helium intensities in these regions.

Both the observations discussed by Brueckner & Bartoe and those obtained with the Harvard ATM instrument on Skylab (Huber *et al.* 1974) show that the He I emission, as well as that of He II, is anomalous in its intensity distribution. Since the contribution function for collisional excitation of the He I 584 Å line peaks at 25000 K, it is clear that the enhancement process must operate at least down to this temperature.

3. The temperature and density structure in coronal holes

In two previous papers (Jordan 1975*a*, 1976) it has been shown that because the distribution of the emission measure, $\int_R N_e^2\,dh$, with temperature, T_e, has a similar shape in quite different regions of the solar atmosphere, the structure above T_0 (*ca.* 200000 K) can be described in terms of P_0, the pressure at T_0, T_c, the maximum isothermal temperature and a, which is related to the emission measure E_m, by

$$E_m = \int_R N_e^2 dh = aT_e^{\frac{3}{2}}. \tag{1}$$

Equation (1) can be rewritten in terms of the temperature gradient,

$$dh/dT = \surd 2\, aT_e^{\frac{5}{2}}/P_e^2. \tag{2}$$

Using also the equation of hydrostatic equilibrium,

$$d(\lg P_e)/dh = -0.86\times 10^{-4}/T_e, \tag{3}$$

one derives

$$[T_c^{\frac{5}{2}} - T_0^{\frac{5}{2}}] = 4.4\times 10^3 P_0^2/a, \tag{4}$$

where T_c is defined either as the temperature at which $P_e \to 0$ or, with the same result, as the temperature at which dT/dh, and hence $F_c \to 0$, where $F_c(T_e)$ is the energy flux carried by thermal conduction. The usual form for $F_c(T_e)$ is used,

$$F_c(T_e) = \kappa T_e^{\frac{5}{2}}\, dT/dh, \tag{5}$$

where κ is the thermal conductivity.

Equation (4) gives a very useful scaling law between T_c (the maximum isothermal temperature that could be observed in for example a particular active region loop), P_0 and a, which can be measured from an absolute line intensity.

The use of (2) and (3) in (5) allows the conductive flux at T_0 – the direction being *back* through the transition region from the corona – to be expressed as

$$F_c(T_0) = 1.6\times 10^{-10}(T_c^{\frac{5}{2}} - T_0^{\frac{5}{2}}). \tag{6}$$

Defining ΔF_R, the radiation loss from a cylinder element as a flux,

$$\Delta F_R = \int_R R_{rad}\, dh \text{ erg cm}^{-2}\text{ s}^{-1},\dagger \tag{7}$$

where

$$R_{rad} = 0.8 N_e^2 P_{rad} \text{ erg cm}^{-3}\text{ s}^{-1}, \tag{8}$$

and, from the calculations by McWhirter *et al.* (1975)

$$P_{rad} = 6.0\times 10^{-17}/T_e \text{ erg cm}^{-3}\text{ s}^{-1} \tag{9}$$

over the range $2\times 10^5\text{ K} < T_e < 10^7$ K, and the use of (2) for dh/dT leads to a total radiative energy loss above T_0 of

$$F_R(T_0) = 1.5\times 10^{-16}\, a(T_c^{\frac{1}{2}} - T_0^{\frac{1}{2}}). \tag{10}$$

The details of the derivation have been given in the previous papers, and are not repeated here.

The observational information on which the method is based is that the quiet Sun emission measure can be described by (1) at temperatures above T_0, i.e. the emission measure gradient is $\frac{3}{2}$. The application to active regions was based on the observation, from the OSO-4 satellite, that up to some temperature T_*, the ratio I_{active}/I_{quiet} is constant, indicating that the emission measure distribution has the same gradient in both quiet and active regions. T_* is the temperature of the average quiet corona, *ca.* 1.5×10^6 K.

Because the energy balance in coronal holes must include the additional term of energy loss in the solar wind, which can be ignored in the closed magnetic field configurations of active region loops, no attempt was made earlier to consider coronal holes by the same method. However, as can be seen above, given the emission measure distribution the method does not depend on any assumption about the relative size of the energy loss terms. Rather, these are determined *from* the emission measure distribution.

The observations of coronal holes made by using the OSO-4 satellite show that $I_{hole}/I_{quiet\ Sun}$ *is* constant, within the error bars up to some temperature, which will be the hole 'coronal' temperature. Figure 3 shows the observed ratios given by Munro & Withbroe (1972) for four regions from the edge to the centre of a coronal hole on the disk. The constant ratio shows that the emission measure distribution has the same shape in a coronal hole as in the quiet Sun, and the formulation previously developed is therefore applicable. The Harvard Skylab data discussed by Rosner & Vaiana (1977) also show a constant ratio up to the coronal hole temperature. Munro & Withbroe made their own analysis of the OSO-4 observations.

† 1 erg $s^{-1} = 10^{-7}$ W.

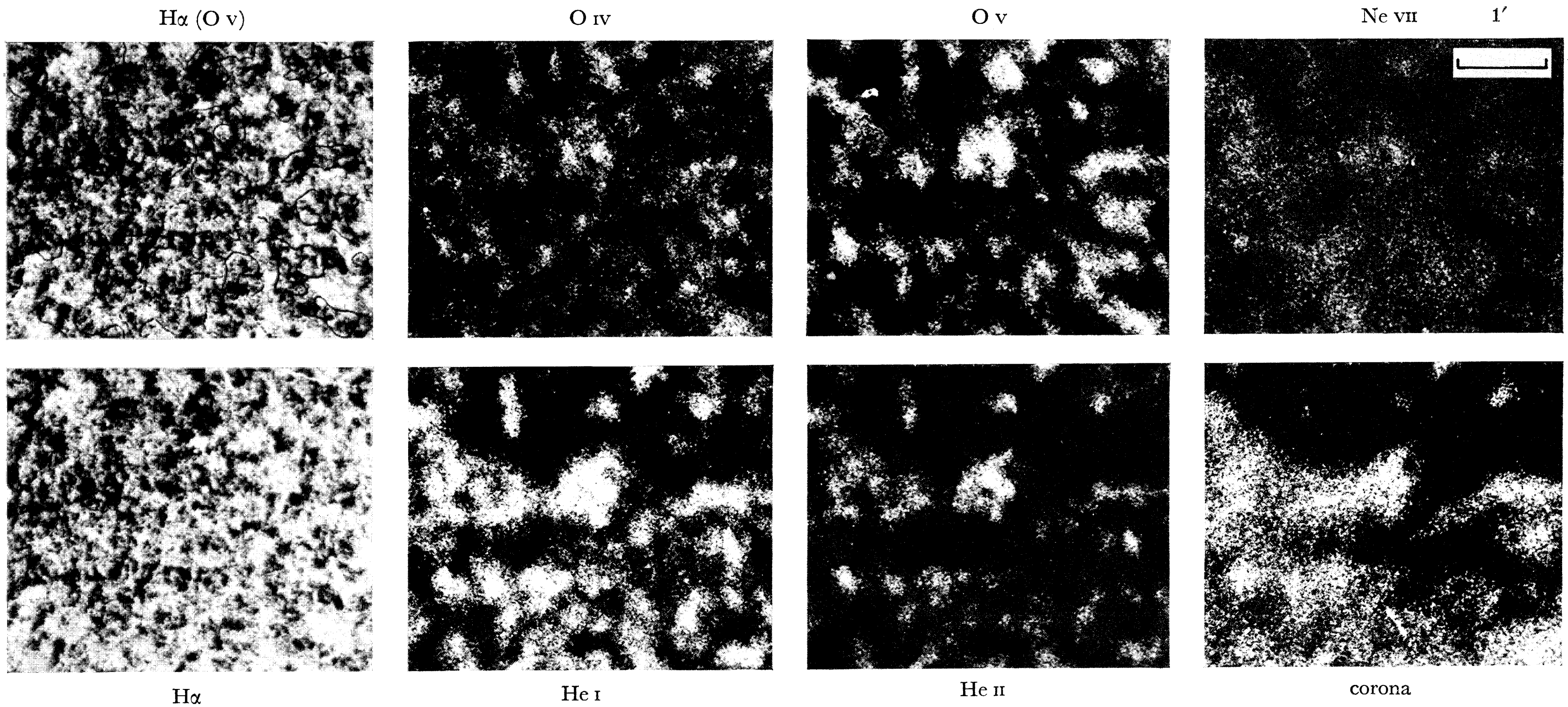

FIGURE 1. A region of the quiet Sun at 12° heliocentric latitude obtained on January 15 1974 from an N.R.L. sounding rocket flight, reproduced from Brueckner & Bartoe (1974) by courtesy of N.R.L. and *Solar Physics*. A coronal hole can be seen in the upper part of the region.

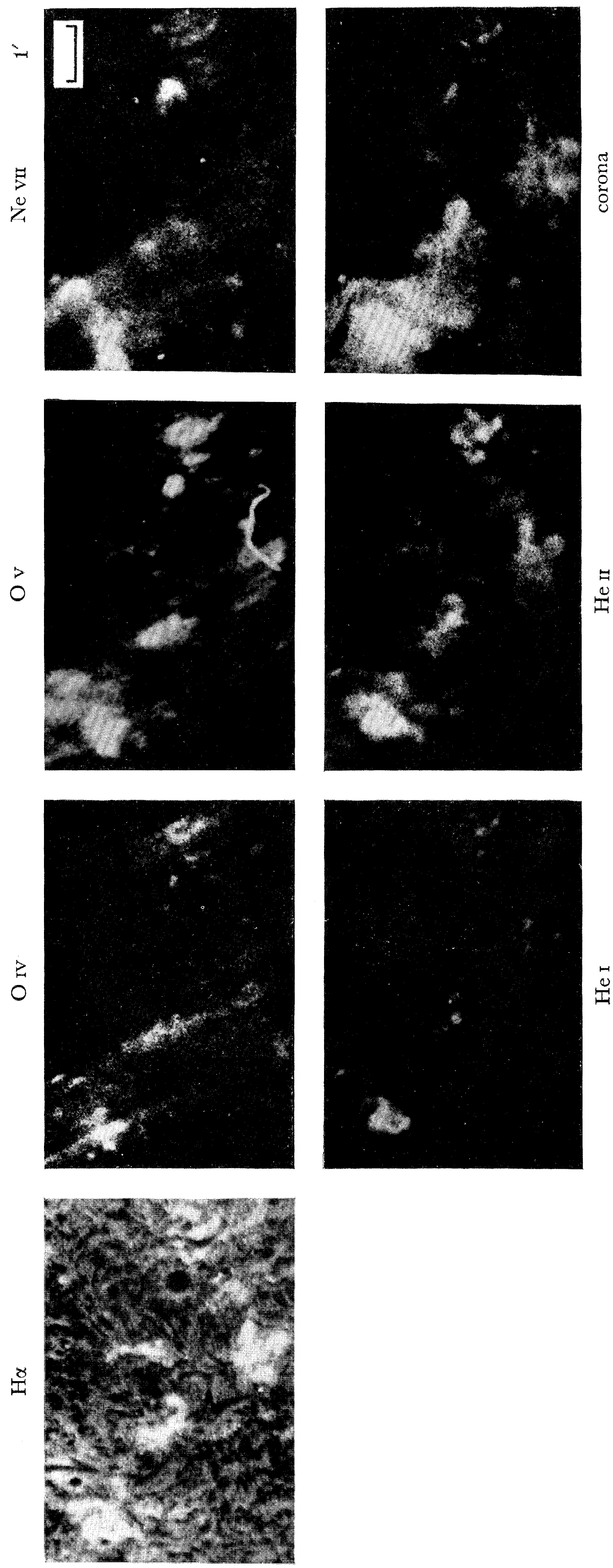

Figure 2. The active regions McMath 706 (upper left) and McMath 703 (lower right), reproduced, as for figure 1, from Brueckner & Bartoe (1974).

PHILOSOPHICAL TRANSACTIONS OF THE ROYAL SOCIETY A MATHEMATICAL, PHYSICAL & ENGINEERING SCIENCES

They found a value of P_e by assuming that the observed Mg x emission was formed over a scale height in an isothermal region at T_{ch}, the coronal hole temperature. Since transition region lines depend on P_e^2 and dh/dT, a self-consistent model can be built up by using the equation of hydrostatic equilibrium. T_{ch} was found from the best fit to the coronal line intensities, and iterations made to give the best fit to both transition region and coronal lines. The method is similar to but not identical with the present one.

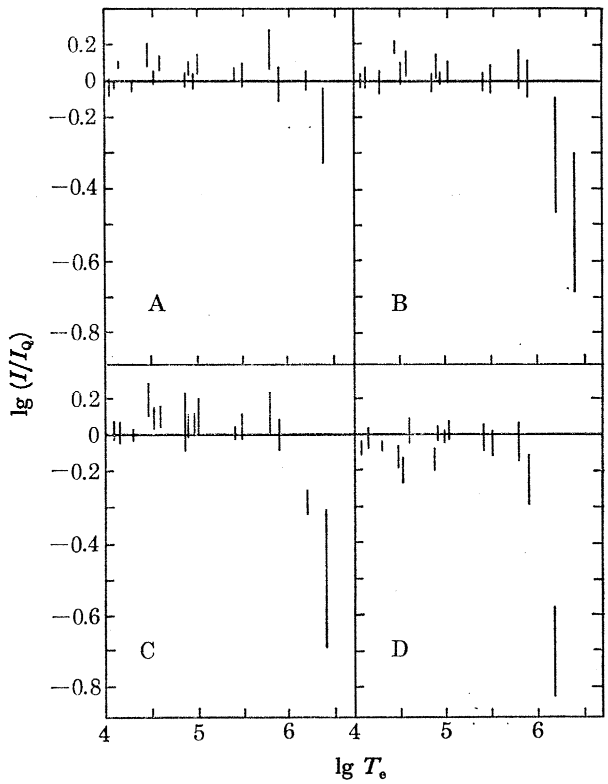

FIGURE 3. Line intensity ratios between regions adjacent to and in a coronal hole, compared with a typical quiet Sun region. The figure is based on one in Munro & Withbroe (1972).

It was from these observations that Munroe & Withbroe deduced that the coronal hole pressure is lower by a factor of three, and the coronal hole temperature gradient is lower by an order of magnitude in comparison with the quiet Sun. Given the same data, the coronal hole parameters can be derived, relative to a chosen standard model, by using (4). The observed relative intensities give the relative values of a in a straightforward manner. Adopting values of $\Delta(\lg P)$ from Munro & Withbroe, $\Delta(\lg T_c)$ can be calculated from (4). Table 1*a* shows the parameters found by Munro & Withbroe, and table 1*b* shows the values of $\Delta(\lg a)$, $\Delta(\lg P)$ and calculated values of lg T_c. It can be seen that the agreement between the two methods is quite good for the first three regions, but that for the last region the results are discordant. However, examination of figure 3 shows that the temperature at which the ratio begins to depart from its previously constant value, and which can be identified with T_c, agrees better with the value given in table 1*b* with Munro & Withbroe's value. Given the low intensity of Mg x in region D it is not surprising that the value of T_c is not well determined. However, the results from the use of the present method support the familiar view of a coronal hole as a region where the pressure is lower, the transition line intensities are marginally lower and T_c is lower. These data show that the conditions depart steadily from those in the quiet corona as regions towards the centre of the hole are examined.

The temperature gradient, given by (2), also decreases steadily towards the centre of the hole. Both the He I emission (Munro & Withbroe 1972) and the He II emission (Reeves & Parkinson 1970) observed from OSO-4 decrease in intensity in the same way.

The energy balance in the hole can now be examined. The values of $F_c(T_0)$ and $F_R(T_0)$ have been found from (6) and (10) and the results are given in table 2, together with their sum $F_T(T_0)$. All three fluxes decrease steadily towards the centre of the hole. However, the ratio F_R/F_c increases towards the centre of the hole but is always less than the value of unity expected with minimum energy loss (see below).

Table 1. Parameters describing properties of coronal holes

	(a) *from Munro & Withbroe* (1972)			(b) *scaling from* $\Delta \lg a$ *and* $\Delta \lg P$, *using equation* (4)		
region	$\lg \{P/(\text{cm}^{-3}\ \text{K})\}$	$\lg (T_c/\text{K})$	$\lg \{F_c/(\text{erg cm}^{-2}\ \text{s}^{-1})\}$	$\Delta \lg a$ (observed)	$\Delta \lg P$ (from (a))	$\lg (T_c/\text{K})$
OSO-4 standard quiet region	14.96	6.22	6.1	0.00	0.00	6.22
quiet region, A	14.90	6.17	6.0	0.00	−0.06	6.17
coronal hole, B	14.84	6.16	6.0	0.00	−0.12	6.12
coronal hole, C	14.77	6.09	5.7	+0.10	−0.19	6.03
coronal hole, D	14.50	6.02	5.1	−0.10	−0.46	5.89

Table 2. Energy loss (ergs per square centimetre per second) from radiation and conduction

region	$\lg F_R(T_0)$	$\lg F_c(T_0)$	$\lg F_T(T_0)$
OSO-4 standard quiet region	5.12	5.75	5.84
quiet region, A	5.08	5.63	5.74
coronal hole, B	5.04	5.50	5.63
coronal hole, C	5.06	5.27	5.48
coronal hole, D	4.73	4.91	5.13

Because coronal holes are not apparent in lines formed at the level of the low chromosphere, it is often assumed that the energy input must be the same as in the quiet Sun. If this were so then because solar wind losses are much smaller than F_c in the quiet Sun, the difference between F_T in quiet Sun and the hole could be attributed to energy lost in the solar wind, F_W. Then F_W would increase towards the centre of the hole and reach a value of 5.6×10^5 erg cm^{-2} s^{-1}. Zirker (1976) quotes a typical value of 5.1×10^5 erg cm^{-2} s^{-1} for the kinetic energy flux of a high-speed solar wind stream, extrapolated back to the solar surface.

From the above it can be seen that if two of the quantities P_0, a or T_c can be determined then the temperature gradient, radiation losses and conduction losses in the quiet Sun and coronal holes can be simply calculated. In the following section, the helium emission enhancement is developed in terms of the same quantities.

To conclude this section, a comparison is made with the work of Hearn (1977) who applied his minimum energy flux hypothesis to this coronal hole. No allowance was made for energy loss in the solar wind in this application, and the main purpose of the discussion below is to show how the scaling laws between P_0, T_c, F_c, etc., arise.

From the sum of $F_c(T_0)$ and $F_R(T_0)$, as given by (6) and (10), F_T, their total, can be expressed in terms of P_0 and a through (4). The minimum energy loss condition is found from $dF_T/da = 0$, i.e. the base pressure is fixed but a and T_c are allowed to vary. The minimum energy loss occurs when $|F_c| = 0.8|F_R|$ since then $dF_c/da = -dF_R/da$. In the present work, F_c and F_R have the same sign.

The scaling law is then

$$aT_c^{\frac{1}{2}} \propto T_c^{\frac{5}{2}}, \tag{11}$$

and also, from (4),

$$T_c \propto P_0^{\frac{4}{9}} \tag{12}$$

and

$$F_T(T_0) \propto P_0^{\frac{10}{9}}. \tag{13}$$

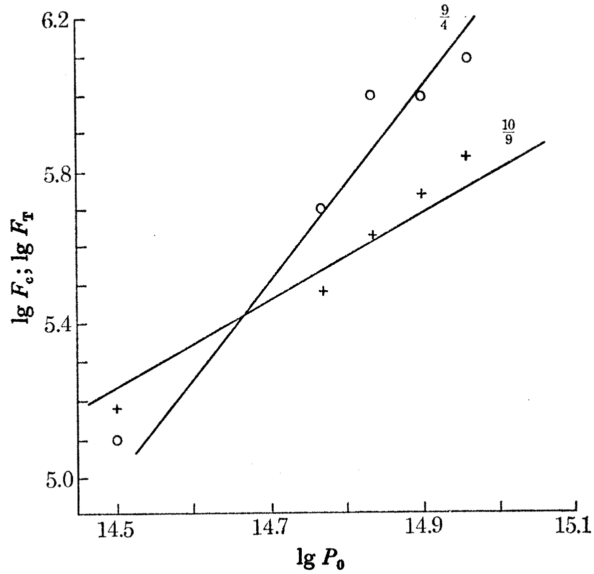

FIGURE 4. The conductive flux, F_c, calculated by Munro & Withbroe (1972) (circles), and the sum of F_c and F_R, the radiative flux, calculated in the present paper (crosses), as a function of P_0, the transition region pressure. See text for discussion of gradients shown.

These scaling laws are identical with those found by Hearn (1977). However, Hearn did not allow F_R and F_c both to be loss terms above T_0, but let F_R balance F_c. Since the sign is not important for the scaling law, it is obvious why the results are the same. An alternative argument can be used to derive the scaling laws (Jordan 1979), which is to say that for a given P_0 the atmosphere can lose energy mainly by radiation or conduction (or indeed solar wind losses). Then since both F_R and F_c must balance the energy input they must have the same dimensions.

It can be seen from table 2 that the ratio F_R/F_c is not constant as would be expected with minimum energy loss, in the absence of a wind.

Figure 4 shows this in another way. The values of lg F_c (as calculated by Munro & Withbroe) are shown as circles, and those of lg F_T (calculated by using the present method), are shown as crosses, both being plotted against lg P_0. Hearn predicts $F_c \propto P_0^{\frac{10}{9}}$ for minimum energy loss and constant κ, the conductivity, which clearly does not fit the circles. However, he argued that a variation in the angle to the radial direction between the quiet Sun and the coronal hole would change κ, and with variable κ but constant energy input he predicts a $\frac{9}{4}$ gradient, which is illustrated.

With the present method it has been found that, although the ratio F_R/F_c varies from feature to feature, the *total* F_R+F_c does fit a $\frac{10}{9}$ gradient. This was found from closed field regions such as active region and flare loops and is discussed by Jordan (1980). However, the result is due more to the insensitivity of the total to the ratio F_R/F_c than to any support for the minimum energy loss hypothesis. Figure 4 shows the $\frac{10}{9}$ minimum energy loss line and the total flux F_T, and it can be seen that in spite of the variation of F_R/F_c the fit looks good.

Hearn's idea that the field geometry is important may well be relevant, but not quite in the way he envisaged. The field geometry must affect the conductive flux, and some calculations for loops with both radial and helical field components have been made by Hood & Priest (1979). In the present method the field is not included explicitly but its effects will be built into the behaviour of the emission measure distribution. The changing value of F_R/F_c from quiet Sun to coronal hole may well be due to, for example, less twisted fields in the coronal hole.

If the minimum energy loss concept, with constant κ, were applied to the present coronal hole data, taking only P_0 as known, it can be seen that although it *would* give a good estimate of F_R+F_c it would systematically underestimate the coronal temperature T_c, and overestimate a, the absolute emission measure.

Since the solar wind is not included in the above it is not worth pursuing the argument further at this stage.

4. Relation between helium emission and non-thermal motions

There now exist many observations of the widths of transition region lines, following the early work by Brueckner & Moe (1973) and Boland *et al.* (1975). Data are now available for particular regions of the atmosphere, e.g. the quiet Sun, coronal holes, sunspots and flares (Doschek *et al.* 1976; Feldman *et al.* 1976; Moe & Nicolas 1976; Feldman *et al.* 1977; Doschek & Feldman 1978). These observations show that the line widths are broader than expected from the electron temperature, that the range of non-thermal velocities is not very large, and that the maximum velocities occur in the region 10^5 to 2×10^5 K. The question of the cause of these motions will be returned to later in this section.

First it is proposed that these non-thermal motions, or the process that causes them, provide the mixing between helium ions formed at one temperature and hotter electrons, and give rise to the enhanced helium emission. The helium enhancement would then be expected to depend on V_T, the non-thermal velocity, on dT/dh and on P_e. One can think either of the non-thermal motions carrying the ions up the steep temperature gradient or of an intermittent penetration down of hotter electrons. The former view will be taken below to show how the enhancement would then depend on V_T, dT/dh and P_0.

The enhancement in emission that would occur if the helium lines were formed at T_f rather than T_i ($T_f > T_i$, where T_i is the temperature expected in ionization equilibrium), is given simply by

$$\frac{I_f}{I_i} = \left(\frac{T_f}{T_i}\right)^{-\frac{1}{2}} \exp\left\{\frac{-W}{k}\left(\frac{1}{T_f}-\frac{1}{T_i}\right)\right\}\frac{N_{ef}}{N_{ei}} \tag{14}$$

through the temperature and density dependence of the collisional excitation rate.

With $P_e = N_e T_e$ and constant pressure,

$$\frac{I_f}{I_i} = \left(\frac{T_i}{T_f}\right)^{\frac{3}{2}} \exp\left\{\frac{W}{k}\left(\frac{1}{T_i}-\frac{1}{T_f}\right)\right\}. \tag{15}$$

It has been assumed that the ion population remains the same.

Now to find T_f a very simple model is taken, following similar arguments used by Shine *et al.* (1975) when discussing the effects of diffusion on the helium emission.

It is assumed that an ion (or clump of ions) travels a distance λ, at velocity V_T before it is collisionally excited after time τ.

Then $$\lambda = v\tau \tag{16}$$

and $$\tau = 1/CN_e, \tag{17}$$

where C is the collisional excitation rate.

TABLE 3. OBSERVED VELOCITIES AND TYPICAL PARAMETER VALUES

region	V_T / km s^{-1}	P_0 / 10^{14} cm^3 K	dT/dh / 10^{-3} K cm^{-1}	$T_f/10^5$ K	I_f/I_i
quiet Sun	25	5.6	12	1.3	5.0
coronal hole	22	3.5	5.4	1.1	3.5
sunspot loop	13	5.6	1.2	0.87	1.4
active region loop	25	28	62	1.3	5.0

The temperature difference $$T_f - T_i = \lambda(dT/dh), \tag{18}$$

which can be written as $$T_f - T_i = V_T(dT/dh)/CN_e. \tag{19}$$

By substituting for C at T_f, with the use of the atomic data in Hearn (1969*b*), equation (19) becomes

$$T_f - T_i = 4.3\times 10^5\, V_T T_f^{\frac{3}{2}} \exp\left(\frac{W}{kT_f}\right)\left(\frac{dT}{dh}\right)\Big/P_e. \tag{20}$$

If T_i is taken as 8×10^4 K, the temperature at which He II has maximum abundance, then T_f can be calculated in terms of V_T, dT/dh and P_0, the same parameters as can be used to describe the structure and energy balance of the particular region of the atmosphere. Some typical numbers are given in table 3. Although not too much should be read into the comparisons given the simple model, it is encouraging that the magnitudes and trend of I_f/I_i are similar to those observed. With this model the He II emission should be closest to its equilibrium value in sunspot loops, where dT/dh is small (Foukal *et al.* 1974), enhanced a little in coronal holes, and more so in the quiet Sun and hot active region loops. Unfortunately, although it is clear from figure 2 that the helium emission is very weak over the sunspot, no quantitative measurement of the O V/He II ratio exists in the literature. The enhancement predicted for the quiet Sun is about that observed, but the coronal hole – quiet Sun contrast is lower than the value of *ca.* 3 found from the composite spectra prepared from the Harvard instrument on Skylab (Vernazza & Reeves 1978). On the other hand, Mango *et al.* (1978) obtain ratios between 1.2 and 1.3.

From the above discussion it can be seen that if the absolute value of the emission measure is known from transition region lines, and either P_0 or T_c can be measured in the same region, then the temperature gradient at T_0 is also known. The helium emission expected in equilibrium conditions can then be predicted and the enhancement of the observed intensity above that calculated can be found. If the non-thermal velocity V_T could also be measured from the transition region lines at *ca.* 10^5 K, then the observed enhancement could be compared with that given by (15) and (20).

If the alternative view of the helium enhancement as being due to intermittent penetration of hot electrons is taken, it is difficult to quantify the enhancement expected. But if as proposed recently (Jordan 1980) the non-thermal motions are a by-product of the deposition of conducted energy, other correlations between the helium enhancement and V_T, P_0 and $\mathrm{d}T/\mathrm{d}h$ should be investigated. In either case the behaviour of the helium emission provides a useful test of models of the dynamic behaviour of the transition region.

The relation between the non-thermal motions and conduction will be briefly discussed. With the formulation given in §3, conduction is a loss term at 2×10^5 K. However, once the emission measure gradient drops below $\frac{3}{2}$, energy is deposited by conduction and cannot immediately be radiated away. This is a long-standing problem, noted, for example, by Giovanelli in 1949. Kuperus & Athay (1976) and Kopp & Kuperus (1968) suggested that the energy deposited might drive motions such as spicules. Bessey & Kuperus (1969) proposed that the resulting motions may resemble detonation waves. If the observed non-thermal motions are identified with the energy flux carried by a propagating wave, such as a sound wave, then a severe problem arises in that the flux of energy carried up appears first to decrease but then to *increase* with T_e above 10^4 K (Boland *et al.* 1975). This problem is removed if the energy that drives the motions originates from energy from conduction *back* at 10^5 K. The turbulent motions can to some degree carry energy down to regions where the radiation is sufficient to dispose of it. A comparison of the energy conducted back at 2×10^5 K in the quiet Sun (*ca.* 4×10^5 erg cm^{-2} s^{-1}) with that radiated below shows that the process must extend down to regions around 10^4 K to dispose of the energy. This is consistent with the beginning of the increase in non-thermal flux at 10^4 K, (see Boland *et al.* 1975), and with the enhancement not only of He II, but also of He I, which should in equilibrium be formed at $T_e \sim 2.5\times10^4$ K. It would also be worth examining the effects of transient excitation on H Ly α, since W/kT_e is also large for this line, and it is usually necessary to introduce a temperature plateau into models to account for its intensity. The enhanced helium emission would itself provide a contribution towards restoring a static energy balance.

It is difficult to say how the atmosphere will in detail respond to the deposition of the conducted energy, but as Moore & Fung (1972), besides others, pointed out, a static solution is apparently not possible. Although the emission line broadening indicates supra-thermal ion velocities, these velocities are less than the sound speed, the proton thermal velocity, and most of the energy will not be in the 'non-thermal' motions. However, on the hypothesis that the observed motions are set up as a result of the deposition of conducted energy, the correlation between $F_c(T_0)$ and V_T has been investigated. (Other scaling laws were also examined.)

If it is supposed that $F_c(T_0) \propto \Phi_T$, where Φ_T is the non-thermal kinetic energy, given by

$$\Phi_T = \rho\langle V_T^2\rangle\, V_T \tag{21}$$

(where ρ is the mass density), then, since

$$F_c(T_0) = \kappa P_0^2 \sqrt{2a} \tag{22}$$

from §3, at $T_e \sim T_0$ the relations

$$V_T^3 \propto P_0/a \propto (\mathrm{d}T/\mathrm{d}h)/P_0 \tag{23}$$

would be expected.

From a limited number of data, particularly those obtained during the slow decay of a flare (Feldman *et al.* 1977), there is support for the scaling law given by (23). It is not inconsistent with the few average quantities given in table 3. Clearly, further tests against observations are required.

As far as the present paper is concerned, the main point to be made is that further analyses of data are required to investigate the correlations between V_T, P_0, dT/dh and the degree of helium enhancement.

5. Conclusions

To account for the intensity of the helium I and II resonance lines, a model is required in which dynamic effects are taken into account. These lines should therefore provide valuable constraints on proposed models. Although the helium lines have been the subject of many calculations, the necessary simultaneous study of other transition region lines has not yet been carried out. To understand the dynamic structure and energy balance in the various atmospheric features, there is clear need for studies of correlations between the non-thermal motions and other atmospheric parameters that can be measured, e.g. the transition region pressure, P_0, coronal temperature, T_c, and the absolute line intensities.

Meanwhile there is some evidence for the hypothesis that the deposition of energy conducted back from the corona drives the observed non-thermal motions, and that the enhancement of the helium emission takes place because of this energy deposition.

References (Jordan)

Athay, R. G. 1960 *Astrophys. J.* **131**, 705.
Athay, R. G. 1965 *Astrophys. J.* **142**, 755.
Athay, R. G. & Johnson, H. R. 1960 *Astrophys. J.* **131**, 413.
Avrett, E. H., Vernazza, J. E. & Linsky, J. L. 1976 *Astrophys. J.* **207**, L199.
Bessey, R. J. & Kuperus, M. 1969 In *Chromosphere–Corona Transition Region*, p. 191. HAO/NCAR.
Boland, B. C., Dyer, E. P., Firth, J. G., Gabriel, A. H., Jones, B. B., Jordan, C., McWhirter, R. W. P., Monk, P. & Turner, R. F. 1975 *Mon. Not. R. astr. Soc.* **171**, 697.
Brueckner, G. E. & Moe, O. L. 1973 *Space research XII*, p. 1595. Berlin-Akademie-Verlag.
Brueckner, G. E. & Bartoe, J.-D. F. 1974 *Sol. Phys.* **38**, 133.
Burton, W. M., Jordan, C., Ridgeley, A. & Wilson, R. 1971 *Phil. Trans. R. Soc. Lond.* A **270**, 81.
Cheng, C. C., Doschek, G. A. & Feldman, U. 1976 *Astrophys. J.* **210**, 836.
Cushman, G. W., Farwell, L., Godden, G. & Rense, W. A. 1975 *J. geophys. Res.* **80**, 482.
Doschek, G. A., Behring, W. E. & Feldman, U. 1974 *Astrophys. J.* **190**, L141.
Doschek, G. A., Feldman, U., Van Hoosier, M. E. & Bartoe, J.-D. F. 1976 *Astrophys. J. Suppl.* **31**, 417.
Doschek, G. A. & Feldman, U. 1978 *Astron. Astrophys.* **69**, 11.
Dupree, A. K. 1972 *Astrophys. J.* **178**, 527.
Dupree, A. K. & Reeves, E. M. 1971 *Astrophys J.* **156**, 599.
Feldman, U. & Behring, W. E. 1974 *Astrophys. J.* **189**, L45.
Feldman, U., Doschek, G. A., Van Hoosier, M. E. & Tousey, R. 1975 *Astrophys. J.* **199**, L67.
Feldman, U., Doschek, G. A., Van Hoosier, M. E. & Purcell, J. D. 1976 *Astrophys. J. Suppl.* **31**, 445.
Feldman, U., Doschek, G. A., Rosenberg, F. U. 1977 *Astrophys. J.* **215**, 652.
Foukal, P. V., Huber, M. C. E., Noyes, R. W., Reeves, E. M., Schmahl, E. J., Timothy, J. G., Vernazza, T. E. & Withbroe, G. L. 1974 *Astrophys. J.* **193**, L143.
Giovanelli, R. G. 1949 *Mon. Not. R. astr. Soc.* **173**, 397.
Goldberg, L. 1939 *Astrophys. J.* **89**, 673.
Hearn, A. G. 1969*a* *Mon. Not. R. astr. Soc.* **142**, 53.
Hearn, A. G. 1969*b* *Mon. Not. R. astr. Soc.* **142**, 259.
Hearn, A. G. 1975 *Astron. Astrophys.* **40**, 355.
Hearn, A. G. 1977 *Sol. Phys.* **51**, 159.
Hirayama, T. 1971 *Sol. Phys.* **19**, 384.
Hood, A. W. & Priest, E. R. 1979 *Astron. Astrophys.* **77**, 233.
Huber, M. C. E., Foukal, P. V., Noyes, R. W., Reeves, E. M., Schmahl, E. J., Timothy, J. E. Vernazza, J. E. & Withbroe, G. L. 1974 *Astrophys. J.* **194**, L115.
Hundhausen, A. J. 1972 In *Coronal expansion and solar wind*, p. 78. Berlin, Heidelberg and New York: Springer-Verlag.
Jordan, C. 1975*a* In *I.A.U. Symposium*, no. 68 (ed. S. R. Kane), p. 109.

Jordan, C. 1975*b* *Mon. Not. R. astr. Soc.* **170**, 429.
Jordan, C. 1976 *Phil. Trans. R. Soc. Lond.* A **281**, 391.
Jordan, C. 1980 *Astron. Astrophys.* (In the press.)
Kohl, J. L. 1977 *Astrophys. J.* **211**, 958.
Kopp, R. A. & Kuperus, M. 1968 *Sol. Phys.* **4**, 212.
Kuperus, M. & Athay, R. G. 1967 *Sol. Phys.* **1**, 361.
Linsky, J. L., Glackin, D. L., Chapman, R. D., Neupert, W. M. & Thomas, R. J. 1976 *Astrophys. J.* **203**, 509.
McWhirter, R. W. P., Thonemann, P. C. & Wilson, R. 1975 *Astron. Astrophys.* **40**, 63.
Mango, S. A., Bohlin, J. D., Glackin, D. L. & Linsky, J. L. 1978 *Astrophys. J.* **220**, 683.
Milkey, R. W. 1975 *Astrophys. J.* **199**, L131.
Milkey, R. W., Heasley, J. N. & Beebe, H. A. 1973 *Astrophys. J.* **186**, 1043.
Moe, O. K. & Nicolas, K. R. 1976 *Astrophys. J.* **211**, 579.
Moore, R. L. & Fung, P. C. 1972 *Sol. Phys.* **23**, 79.
Munro, R. H. & Withbroe, G. L. 1972 *Astrophys. J.* **176**, 511.
Noyes, R. W., Foukal, P. V., Huber, M. C. E., Reeves, E. M., Schmahl, E. J., Timothy, J. G., Vernazza, J. E. & Withbroe, G. L. 1975 In *I.A.U. Symposium*, no. 68 (ed. S. R. Kane), p. 3.
Noyes, R. W., Withbroe, G. L. & Kirschner, R. P. 1970 *Sol. Phys.* **11**, 388.
Pottasch, S. R. 1964 *Space Sci. Rev.* **3**, 816.
Reeves, E. M. & Parkinson, W. H. 1970 *Astrophys. J. Suppl.* **21**, 1.
Rosner, R. & Vaiana, G. S. 1977 *Astrophys. J.* **216**, 141.
Shine, R. A., Gerola, H. & Linsky, J. L. 1975 *Astrophys. J.* **202**, L101.
Tousey, R. 1967 *Astrophys. J.* **149**, 239.
Tousey, R., Bartoe, J.-D. F., Bohlin, J. D., Brueckner, G. E. Purcell, J. D., Scherrer, V. E., Schumacher, R. J., Sheeley, M. R. & Van Hoosier, M. E. 1973 *Sol. Phys.* **33**, 265.
Vernazza, J. E., Avrett, E. H. & Loeser, R. 1973 *Astrophys. J.* **184**, 605.
Vernazza, J. E. & Reeves, E. M. 1978 *Astrophys. J.* **37**, 508.
Zirin, H. 1969 *Sol. Phys.* **9**, 77.
Zirin, H. 1975 *Astrophys. J.* **199**, L63.
Zirker, J. B. 1976 *I.A.U. Colloquium* no. 36 (ed. R. M. Bonnet & P. Delache), p. 421.

PHILOSOPHICAL TRANSACTIONS OF THE ROYAL SOCIETY A MATHEMATICAL, PHYSICAL & ENGINEERING SCIENCES

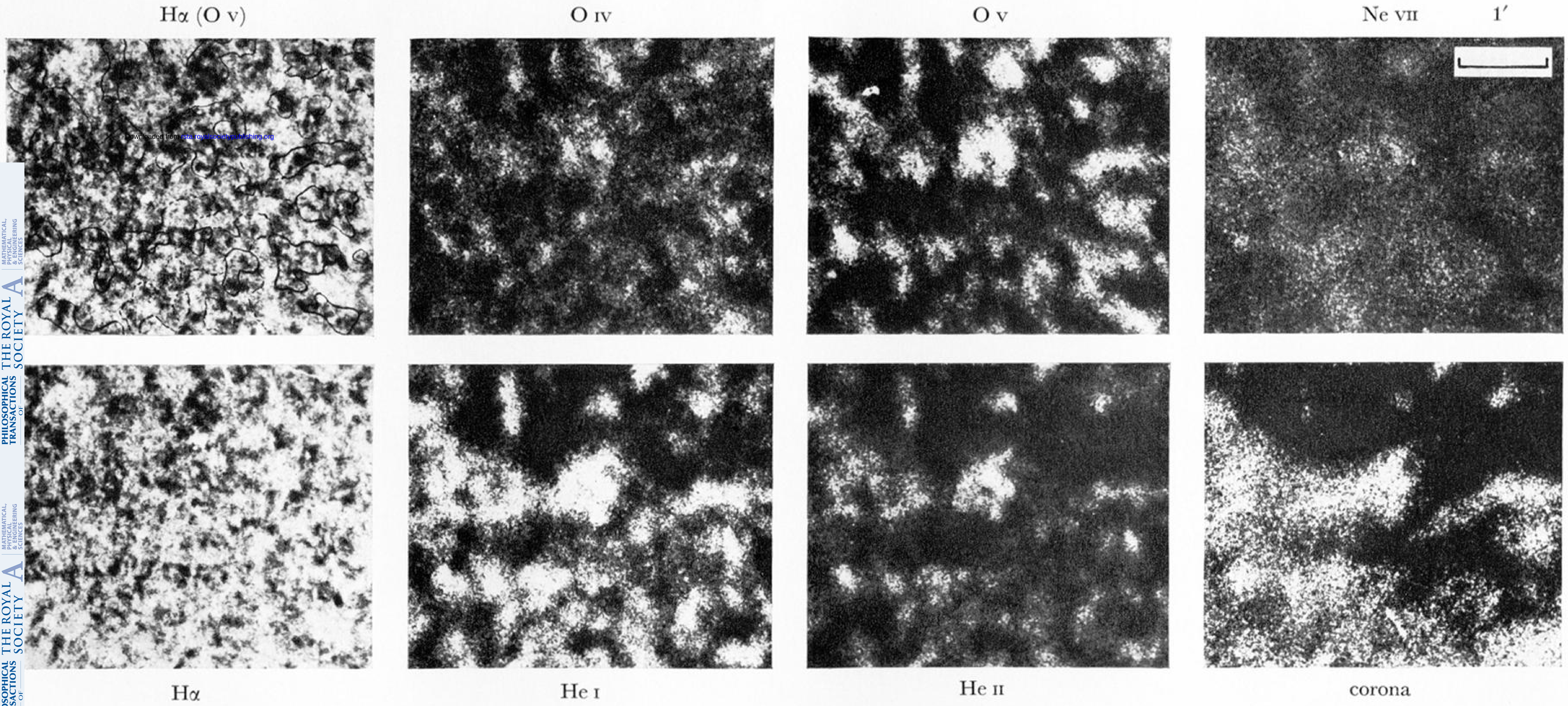

FIGURE 1. A region of the quiet Sun at 12° heliocentric latitude obtained on January 15 1974 from an N.R.L. sounding rocket flight, reproduced from Brueckner & Bartoe (1974) by courtesy of N.R.L. and *Solar Physics*. A coronal hole can be seen in the upper part of the region.

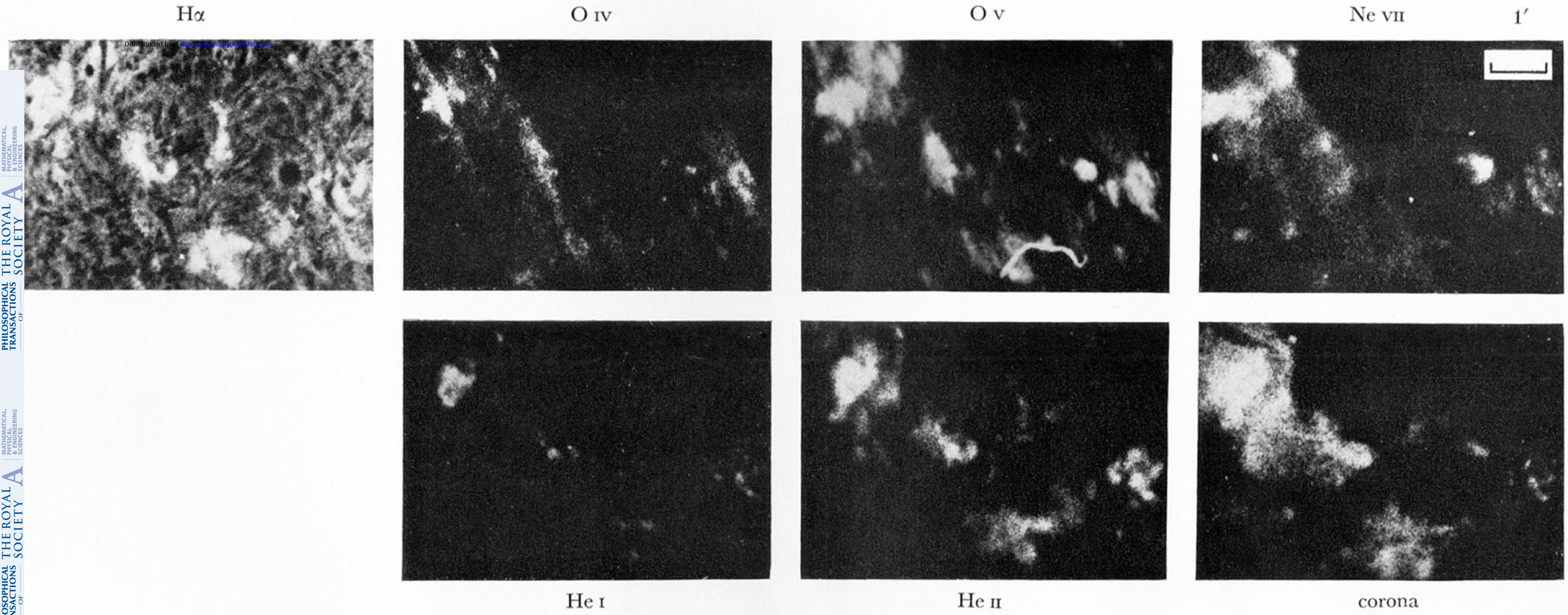

FIGURE 2. The active regions McMath 706 (upper left) and McMath 703 (lower right), reproduced, as for figure 1, from Brueckner & Bartoe (1974).